

DOI: 10.1002/cplu.201300276

“Clicking” Porphyrins to Magnetic Nanoparticles for Photodynamic Therapy

Merlyn Thandu,^[a] Valentina Rapozzi,^[c] Luigi Xodo,^[c] Fernando Albericio,^{*,[b, d, e]}
Clara Comuzzi,^{*,[a]} and Silvia Cavalli^{*,[a, b, f]}

A method for the preparation of superparamagnetic iron oxide nanoparticle–porphyrin (SPION-TPP) conjugates through click chemistry, which can be used as novel theranostic nanoagents for photodynamic therapy is developed. The synthesis, characterisation, and evaluation of the photocytotoxicity profiles of the nanoconjugates prepared is reported. Upon light irradiation, SPION-TPP nanoconstructs promote a photodynamic effect in vitro in murine amelanotic melanoma B78-H1 cells, with IC₅₀ values in the region of 800 nm, similarly to unbound TPP, whereas they remain non-cytotoxic in the dark. However, these nanoconstructs show poor cellular uptake, which influen-

ces a linear dose–response effect. Therefore, the improvement of delivery to cells has also been studied by conjugating a well-known cell-penetrating peptide (TAT peptide) to the SPION-TPP nanoparticles. The new nanoconstructs show lower IC₅₀ values (in the region of 500 nm) and a clear dose–response effect. Our results suggest that TAT-conjugated SPION-TPP nanoparticles are efficient nanodevices both for tracking drugs by means of magnetic resonance imaging (MRI)-based techniques and for treating cancer cells through photodynamic therapy, thus functioning as promising theranostic nanoagents.

Introduction

Advances in nanotechnology have led to new opportunities for the detection, cure, and post-treatment monitoring of cancer.^[1] In this regard, theranostic nanoagents are advanced tools in nanomedicine; they combine drugs and probes within the same nanostructure, and thus, have unique potential in

promoting the simultaneous treatment and diagnosis of diseases, as well as determining the distribution, release, and therapeutic efficacy of a drug.^[2] Theranostics based on engineered superparamagnetic iron oxide nanoparticles (SPIONs) are particularly interesting. Because of their superparamagnetic character, SPIONs can be used as negative contrast agents in magnetic resonance imaging (MRI).^[2,3] Furthermore, upon functionalisation of SPIONs with fluorescent dyes, they can act as bimodal nanodevices for both magnetic resonance and fluorescence microscopy imaging.^[4] Moreover, they can be used for hyperthermia therapy (HT),^[2a] a technique in which the magnetic particles are heated selectively by applying a high-frequency magnetic field and then used to achieve thermal ablation of tumours, or as magnetic vectors that can be directed to a specific target by exploiting a magnetic field gradient.^[5]

Photodynamic therapy (PDT) is a local clinical treatment of cancers, and is particularly efficient in the case of skin tumours. PDT involves three nontoxic components: a photosensitiser, light, and oxygen.^[6] In combination, these elements give rise to cytotoxic oxygen species such as singlet oxygen, which result in cell death. In this medical practice, photosensitising molecules play a crucial role in generating singlet oxygen after light irradiation to cause oxidative damage, which leads to the death of malignant cells.^[7] Porphyrins and their derivatives have been studied extensively as powerful photosensitisers. Their unique photophysical and photochemical properties and presence in natural systems make them an attractive choice for the generation of singlet oxygen in PDT.^[8] Some commercially available porphyrins (e.g., Photofrin) are already used for tumour treatment.^[7a,9] There is great research interest in the

[a] M. Thandu, Dr. C. Comuzzi, Dr. S. Cavalli
Department of Chemistry, Physics and Environment
University of Udine
Via del Cottonificio 108, 33100 Udine (Italy)
E-mail: clara.comuzzi@uniud.it

[b] Prof. Dr. F. Albericio, Dr. S. Cavalli
CIBER-BBN
Networking Centre on Bioengineering, Biomaterials, and Nanomedicine
Institute for Research in Biomedicine (IRB-Barcelona)
Baldiri Reixac 10, 08028 Barcelona (Spain)
E-mail: albericio@irbbarcelona.org

[c] Dr. V. Rapozzi, Prof. Dr. L. Xodo
Department of Medical and Biological Sciences
School of Medicine, University of Udine
Piazzale Kolbe 4, 33100 Udine (Italy)

[d] Prof. Dr. F. Albericio
Department of Organic Chemistry
University of Barcelona, 08028 Barcelona (Spain)

[e] Prof. Dr. F. Albericio
School of Chemistry and Physics
University of KwaZulu-Natal, 4001 Durban (South Africa)

[f] Dr. S. Cavalli
Current address:
Center for Advanced Biomaterials for Health Care IIT@CRIB
Istituto Italiano di Tecnologia
Largo Barsanti e Matteucci 53
80125 Naples (Italy)
E-mail: silvia.cavalli@iit.it

 Supporting information for this article is available on the WWW under <http://dx.doi.org/10.1002/cplu.201300276>.

possibility of synthesising novel porphyrin derivatives for use in targeted tumour therapy and diagnosis (theranostics).^[10] Another important feature of novel photosensitisers is their capacity to absorb at wavelengths in the red region, which is most penetrating in living tissue (therapeutic window).^[11] Furthermore, numerous methodologies for active targeting have been developed to increase the efficacy of photosensitisers, such as their conjugation to peptides or antibodies.^[12] PDT agents have also been encapsulated within polymers to yield higher local concentrations at target sites.^[13] Nanoparticles have also been used to enhance the delivery of hydrophobic photosensitisers.^[14] For example, the conjugation of porphyrins to magnetic nanoparticles has been shown to increase their cellular uptake. Moreover, porphyrins are combined with biological vectors such as proteins, steroids, toxins, carbohydrates, peptides and functionalised nanoparticles to overcome the problem of systemic prolonged photosensitisation syndrome shown by healthy tissues.^[15]

The so-called “click” reaction, or copper(I)-catalysed Huisgen 1,3-dipolar cycloaddition, is of considerable relevance as a conjugation method for a wide range of biomolecular applications because of the unreactive nature of both azides and alkynes towards functional groups that are present in biomolecules.^[16] Moreover, the thermal and hydrolytic stability of the cycloaddition product is of great interest in the field of bioconjugation. In addition to the chemoselectivity and stability of the “click” reaction, it is also particularly interesting that it occurs efficiently in aqueous media at room temperature and with high selectivity, as only the 1,5-substituted triazole is formed. This technique has been used extensively for a broad range of bioconjugations such as the preparation of drug-delivery nanosystems,^[17] biomaterials,^[18] and radiopharmaceutical drugs.^[19] The “click” reaction has also been used in the specific field of porphyrin synthesis and for the binding of these compounds to materials.^[20] Moreover, azido-modified nanoparticles have been prepared for general labelling through “click” chemistry.^[21]

Here, we report the synthesis and characterisation of nanoconjugates between SPIONs and a porphyrin (a derivative of tetraphenylporphyrin, abbreviated as TPP in the text). Conjugation was achieved by exploiting copper(I)-mediated “click” chemistry. In this way, a new nanoconstruct (here abbreviated as SPION-TPP), which can act as an imaging probe (e.g., contrast agents for MRI) as well as a therapeutic drug for anticancer PDT, was prepared. We anticipate that the conjugation of a cell-penetrating peptide (CPP) to nanoparticles bearing the photosensitisers may lower the IC₅₀ values by improving their cellular uptake.^[22] Therefore, a CPP was also conjugated to the SPION-TPPs to improve delivery to cells. For this reason, a more advanced nanoconstruct (here abbreviated as Rhod-TAT-SPION-TPP) was prepared by first functionalising SPIONs with a well-known CPP (a derived sequence of TAT peptide functionalised with rhodamine). For this conjugation, we used a protocol based on the aniline-catalysed oximation described previously by our group for similar purposes.^[23] Subsequently, the Rhod-TAT-SPIONs were linked to TPP through “click chemistry”, as in the case of the SPION-TPP nanoparticles. Moreover, through exploitation of the rhodamine inserted in the TAT se-

quence, Rhod-TAT-SPION-TPP nanoagents could also be used as probes for confocal microscopy, and allow for the subcellular localisation of the photosensitiser magnetic nanoparticles. The efficiency of singlet oxygen production upon light irradiation was studied through UV/Vis spectroscopy and compared to that of the unbound TPP derivative. Subsequently, detailed biological studies were conducted to evaluate the cytotoxicity and cellular uptake of the new synthesised nanoconstructs to validate them as useful theranostics for photodynamic therapy.

Results and Discussion

Synthesis and characterisation

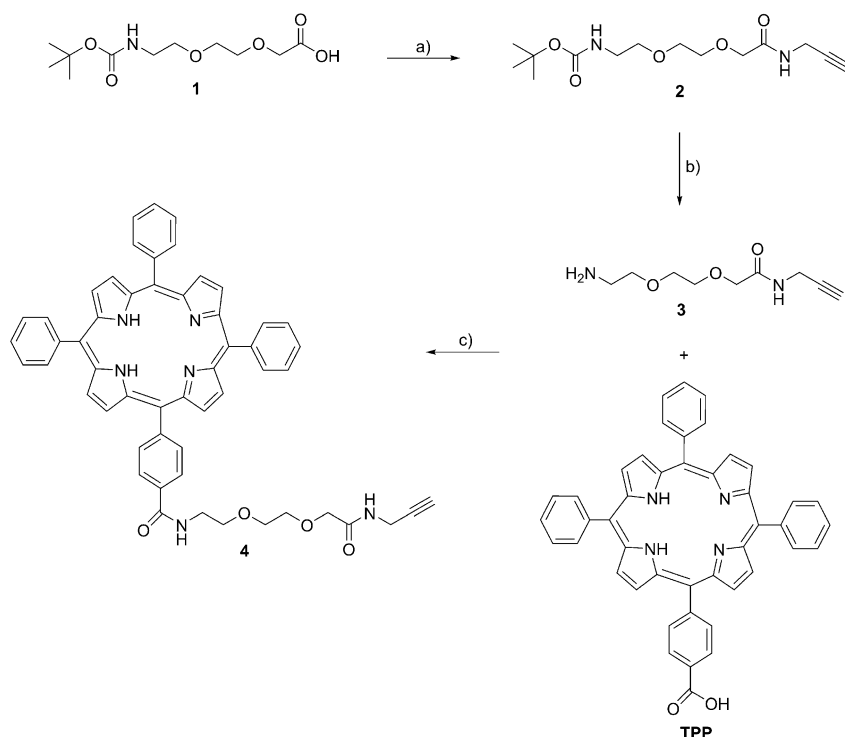
A short ethylene glycol derivative of TPP (compound **4** in Scheme 1) was synthesised to increase the water affinity of the photosensitiser and favour its conjugation to SPION through “click chemistry” in buffer media.

In the first step of the synthesis, propargyl amine was reacted to commercially available 2-[2-(Boc-amino)ethoxy]ethoxyacetic acid (dicyclohexylammonium salt) with *N*-(3-dimethylaminopropyl)-*N*-ethylcarbodiimide (EDC), 1-hydroxybenzotriazole (HOBT) and triethylamine (TEA) in anhydrous dichloromethane (DCM). The condensed product was then treated with a 1:1 (v/v) solution of trifluoroacetic acid (TFA) in DCM to remove the Boc protecting group. Subsequently, the product was reacted directly with TPP using similar reaction conditions to those in the first step of the synthesis.

Commercially available SPION-NH₂ nanoparticles were functionalised with the NHS ester of 12-azido-4,7,10-trioxadodecanoic acid in citrate buffer (pH 8) containing 10 μL of diisopropylethylamine (DIPEA), as shown in Scheme 2.^[21b] “Click” chemistry was employed to conjugate the TPP derivative **4** to azido-functionalised SPION (SPION-N₃). Samples were prepared in phosphate buffer at pH 7.5 by using 0.5 equivalents of CuSO₄·5H₂O and 2 equivalents of Na ascorbate to reduce in situ copper(II) to copper(I), the effective catalyst in the reaction. After overnight rotation to ensure good mixing of the colloidal dispersion, the samples were dialysed first against water containing 10 mM EDTA to remove copper salt traces, and subsequently against deionised water. A final dialysis against PBS was performed in the case of samples used for the biological experiments. Although copper cations were shown to be easily complexed by porphyrins,^[20c] we did not observe interference with the “click” reaction under our experimental conditions.

Analysis

UV/Vis spectroscopy of the nanoconjugate solutions after dialysis showed the occurrence of the Soret band characteristic of the porphyrin (418 nm), whereas no UV absorbance was observed in the control samples in which no catalyst was added (data not shown). Furthermore, the occurrence of the reaction could be checked easily, as upon conjugation, the four Q bands of the free TPP (at 515, 548, 585, and 641 nm) collapsed into only one Q band centred at 538 nm (see Supporting Information, Figure S1 A and D), whereas the Soret band (422 nm)



Scheme 1. Synthesis of TPP derivative **4**. A) 1.2 equiv EDC, 1.2 equiv HOBT-H₂O, and 2 equiv TEA in dry DCM, stirred 5 min; 1.2 equiv propargyl amine added and stirred at RT overnight. B) 1:1 (v/v) of TFA in DCM. C) 10 mg of TPP, 1.5 equiv EDC, 1.5 equiv HOBT-H₂O and 2 equiv TEA in dry DCM, stirred 5 min; 1.5 equiv compound **3** added and stirred at RT overnight.

did not shift significantly compared to that of free TPP. The porphyrin loading on the SPIONs was obtained spectrophotometrically through two methods, as described in the Experimental section and Supporting Information (Figure S1C and D).

The incidence of the reaction and the formation of the triazole ring upon conjugation was also verified through ¹H high-resolution magic angle spinning (HRMAS) NMR spectroscopy.^[24] As shown in the NMR spectrum in Figure 1, the CH of the triazole was identified as the singlet peak at 9.40 ppm. Furthermore, as expected, the peaks of the pyrrole and phenyl groups related to the porphyrin molecule were observed in the aromatic region (from 7.19 to 8.71 ppm) and at negative ppm (−2.98 ppm). Finally, the peaks related to the CH₂O group of the short ethylene glycol linker were found between 4.39 and 4.82 ppm. The remaining peaks (0.5–4 ppm) were ascribed to the dextran-coated SPION and to the deuterated DMSO used as solvent for the NMR experiments (in addition, the usual broad peak of water related to the solvent was found at around 3.4 ppm). No porphyrin-related peaks were found in the control ¹H HRMAS NMR of SPION-N₃ (see Figure S2 in Supporting Information).

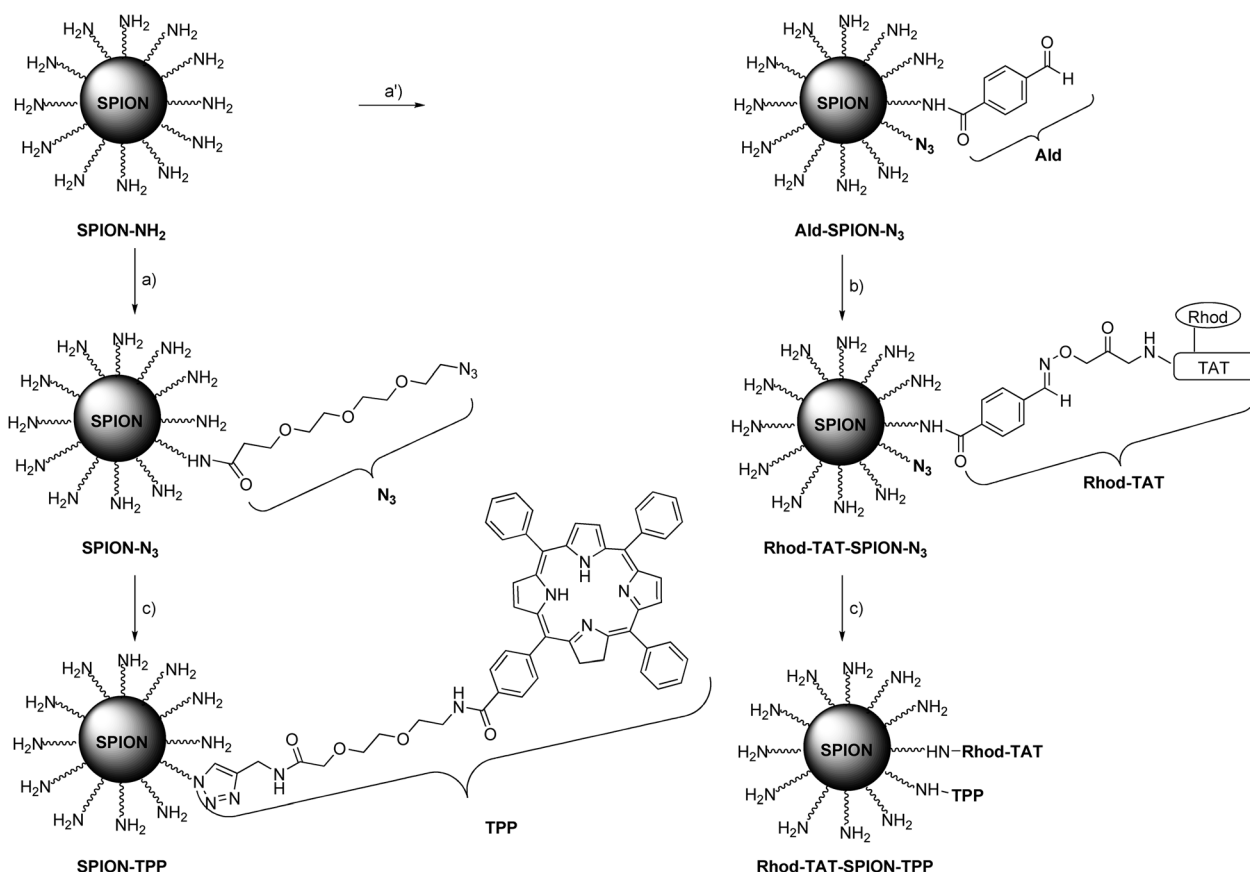
The capability of SPION-TPP conjugates to generate singlet oxygen, the key toxic species that provokes the photokilling effect in PDT, was evaluated through an anthracene-9,10-dipropionic acid (ADPA) test,^[14a,25] and was compared to that of the commercially available porphyrin (5-(4-carboxyphenyl)-10,15,20-triphenyl-21H,23H-porphyrin; TPP). The conjugation

of TPP to the SPION did not alter the ¹O₂ production of unbound TPP (see Figure 2).

With the aim of improving cellular uptake and studying the cellular internalisation of the SPION-TPP conjugates, we also prepared a more advanced type of nanostructure, Rhod-TAT-SPION-TPP, by conjugating SPION-TPP to a cell-penetrating peptide (CPP). As the CPP, we used the HIV TAT-derived sequence: a small basic peptide (RKKRRQRRR) that has been shown to deliver a variety of cargoes into cells.^[26] SPIONs were loaded with both benzaldehyde and azide (Ald-SPION-N₃) reacting groups, as shown in Scheme 2. Ald-SPION-N₃ nanoconjugates were first reacted with an amino-oxycetyl-derived peptide sequence of TAT (functionalised with rhodamine, Rhod-TAT), following a protocol that we described previously.^[23] After dialysis of the Rhod-TAT-SPION conjugate against water,

the TPP derivative **4** was also introduced through “click” chemistry, as described in the text.

The photoactivity of the nanoconjugates was evaluated in murine amelanotic melanoma B78-H1 cells. The cells were incubated with SPION-TPP or Rhod-TAT-SPION-TPP at different concentrations for 3 h, under conditions of 37 °C and 5% CO₂, and subsequently illuminated with a white halogen lamp at a fluence of 14 J cm^{−2}. First, resazurin assays were conducted at two concentrations (400 and 800 nm) of SPION-TPP (Figure 3A). Upon light irradiation, the SPION-TPP nanoconstructs reduced the metabolic activity of the B78-H1 cells up to almost 50% compared with the control (nanoparticles without porphyrin, SPION-NH₂). From this experiment, an IC₅₀ value of about 800 nm can be estimated. As expected, B78-H1 cells treated with SPION-TPP, but not irradiated with light, did not show any reduction in metabolic activity, demonstrating that the nanoparticles were not bioactive or cytotoxic in the dark (at least at the concentrations used). As anticipated from the singlet-oxygen generation test, the bioactivity of SPION-TPP nanoparticles was comparable to that of TPP alone (see Figure S3 in Supporting Information). However, we did not observe a clear linear dose–response effect with SPION-TPP (data not shown). This observation may be attributed to poor cellular uptake of the nanoparticles and their consequent aggregation outside the cell membrane. In light of these results, we decided to increase the uptake of the SPION-TPP nanoparticles by conjugating them to the HIV TAT-derived sequence. In the case of this new nanoconstruct (Rhod-TAT-SPION-TPP), we



Scheme 2. Synthesis of SPION-TPP and Rhod-TAT-SPION-TPP nanoconjugates: A) 5 mg *N*-hydroxysuccinimidyl ester of 12-azido-4,7,10-trioxadodecanoic acid, 10 μ L DIPEA in 0.1 M citrate buffer at pH 8, rotated overnight at RT. A') 5 mg *N*-hydroxysuccinimidyl ester of 12-azido-4,7,10-trioxadodecanoic acid, 4 mg *N*-hydroxysuccinimidyl ester of 4-formylbenzoic acid, 10 μ L DIPEA in 0.1 M citrate buffer at pH 8, rotated overnight at RT. B) 2 mg amino-oxyacetyl-derived Rhod-TAT peptide, 100 mM aniline in 0.1 M phosphate buffer at pH 7.5, rotated overnight at RT in dark. C) 2 mg TPP derivative 4, 0.5 equiv. CuSO₄·5H₂O, 10 equiv. sodium ascorbate in 0.1 M phosphate buffer at pH 7.5, rotated overnight at RT (in dark if rhodamine present).

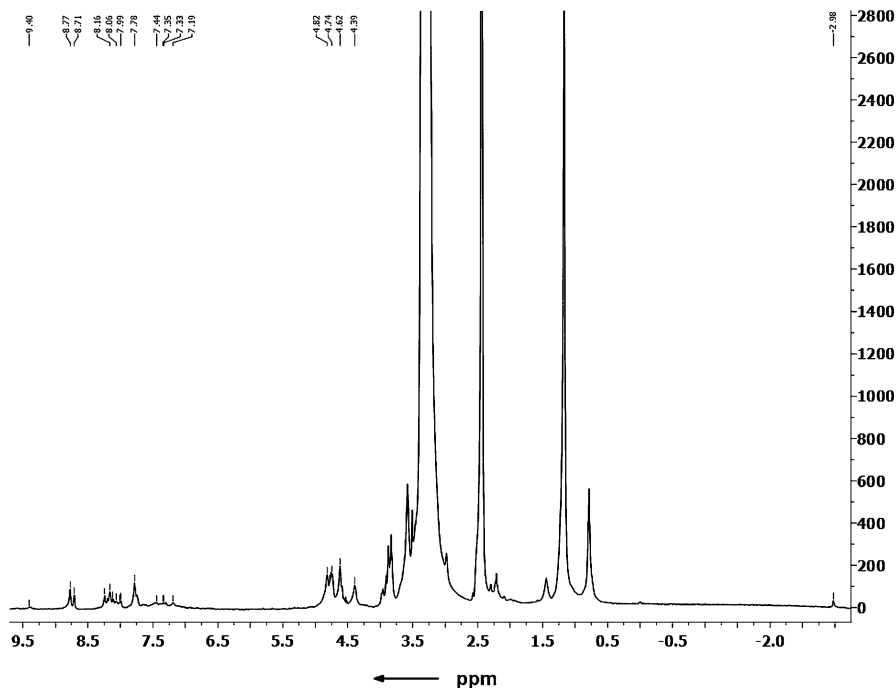


Figure 1. ¹H HRMAS-NMR of SPION-TPP. 2 mg of lyophilised nanoconjugate powder was dispersed in 60 μ L of deuterated DMSO (1024 scans at RT).

indeed observed a linear dose-response reduction in metabolic activity as well as a lower IC₅₀ value (about 500 nM) compared with that for SPION-TPP (Figure 3B). As expected, the Rhod-TAT-SPION-TPP was not cytotoxic in the dark (Figure 3C).

To gain insight into the photokilling mechanism triggered by the designed compounds, we studied the photodynamically treated B78-H1 cells stained with annexin V and propidium iodide (PI), through fluorescence-activated cell sorting (FACS) analysis. In early apoptosis, cell membranes are known to lose their phospholipid asymmetry, and phosphatidyl serine (PS), which is normally located in the inner leaflet, redistributes to the outer leaflet. Because annexin V shows a high affinity for PS, annexin V-

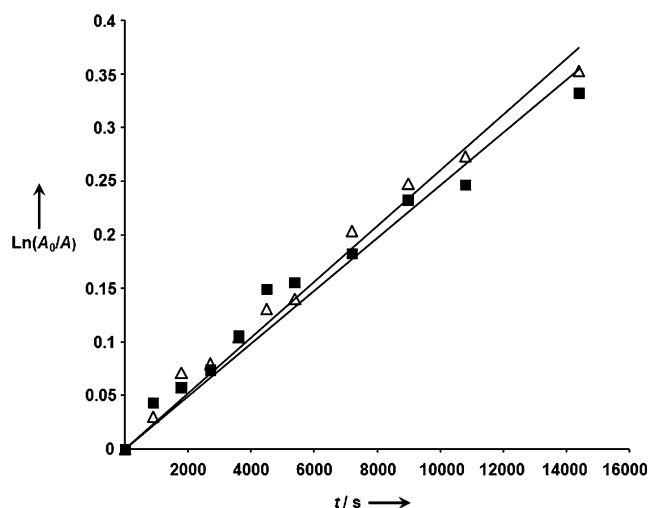


Figure 2. Photo-oxidation of anthracene-9,10-dipropionic acid (ADPA). Experiment conducted by exposing solutions containing ADPA and photosensitisers to light (60 W) for different durations. The absorbance decay, caused by $^1\text{O}_2$ oxidation of ADPA, is reported as $\ln A_0/A^{-1}$ vs. t (s). A_0 is the ADPA absorbance at 455 nm at $t=0$, and A is the ADPA absorbance at 455 nm at $t=1-10$, corresponding to 900, 1800, 2700, 3600, 4500, 5400, 7200, 9000, 10800, and 14400 s, respectively. The treated solutions were: A) 73 μM ADPA and 0.5 μM 5-(4-carboxyphenyl)-10,15,20-triphenyl-21 H,23 H-porphyrin (TPP) in PBS (black squares); and B) 73 μM ADPA and 0.5 μM SPION-TPP in PBS (white triangles). TPP contents were calculated according to the UV/Vis data by applying the method described in the experimental part.

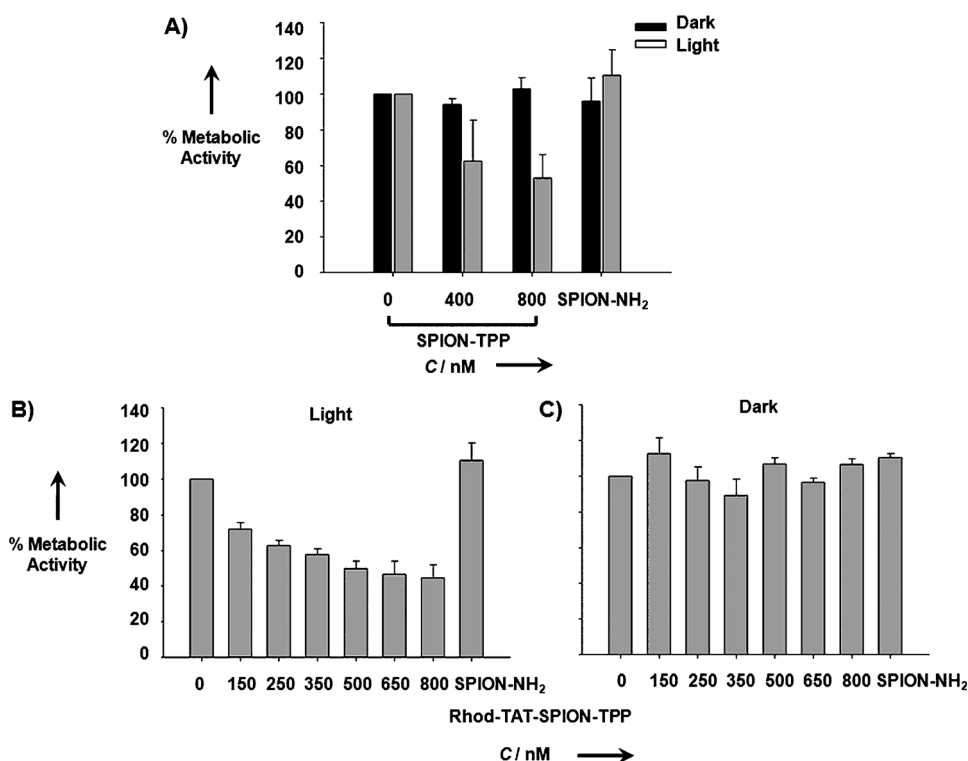


Figure 3. Phototoxicity of SPION-TPP and Rhod-TAT-SPION-TPP nanoconjugates. Resazurin viability test with B78-H1 cells. Cells were incubated for 3 h at 37 °C and 5% CO_2 using increasing concentrations of TPP conjugated to the nanoparticles (TPP contents were calculated according to the UV/Vis data by applying the method described in the experimental part). One set of cells was illuminated with a white halogen lamp at 14 J cm^{-2} , and another set was kept in the dark. Resazurin was added after 23 h, and the readout was obtained 24 h after illumination.

FITC can mark cells in early apoptosis. In contrast, necrotic cells, which are permeable to both annexin V and PI, are stained by the two dyes.^[27]

Figure 4 shows that the treatment of B78-H1 cells with 400 nM SPION-TPP increased the fraction of early apoptotic and necrotic cells compared with untreated cells (apoptotic cells from 2.23% to 17.51%; necrotic cells from 2.09% to 7.9%). However, upon treatment of cells with 400 nm of Rhod-TAT-SPION-TPP nanoparticles, the sum of the fraction of necrotic and apoptotic cells increased up to 35.42%, whereas with SPION-TPP, the same fraction increased only to 25.41%. TPP concentrations below IC_{50} values were selected to observe all possible cell populations (healthy, necrotic, and apoptotic cells). These data demonstrated that TAT conjugation was an efficient strategy for enhancing the efficacy of the SPION-TPP nanoparticles and decreasing the metabolic activity, and thus the proliferation, of the B78-H1 cells. This enhancement is probably caused by a TAT-mediated increase in nanoparticle cellular uptake. The efficient uptake of Rhod-TAT-SPION-TPP could also be visualised in the FACS experiments reported in Figure 4D. Given that rhodamine dye, which is present on the TAT peptide conjugated to the nanoparticles, absorbs in the red region (567 nm), the FACS plots showed that the whole cell population was shifted to this region (upwards along the y-axis, in comparison to the bottom left panels), indicating that all the cells had indeed incorporated Rhod-TAT-SPION-TPP nanoparticles.

To corroborate this observation, we performed confocal microscopy measurements with Rhod-TAT-SPION-TPP nanoparticles. Figure 5 shows that the Rhod-TAT-bearing nanoparticles were taken up quickly by the cells; after incubation for 3 h, the cytoplasm of the cells was strongly stained red owing to the rhodamine fluorescence. Furthermore, we found that nanoparticles were still present inside the cells even 24 h after delivery.

Conclusion

We have described a synthetic route for the preparation of superparamagnetic iron oxide-porphyrin (SPION-TPP) conjugates through “click” chemistry. We have also reported the characterisation and evaluation of the phototoxicity of the designed nanoconjugates. Our results showed that upon light irradiation, SPION-TPP nanoconstructs promoted a photodynamic effect in murine amelanotic mel-

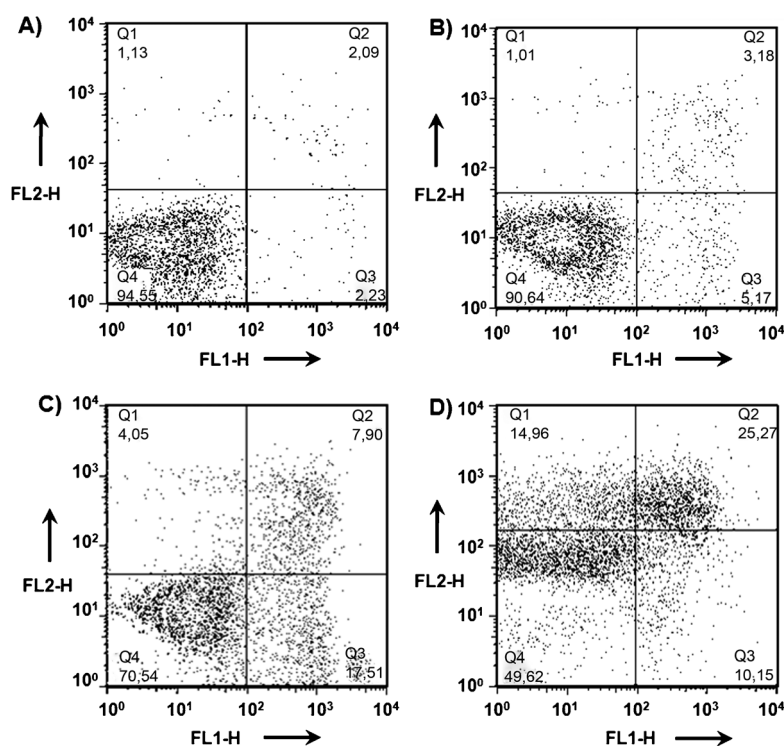


Figure 4. FACS analysis of B78-H1 cells treated photodynamically with SPION-TPP and Rhod-TAT-SPION-TPP and stained with annexin V-FITC and PI. B78-H1 cells were plated at a density of 5×10^5 cells in a 6-well plate. After 24 h, the cells were A) untreated, B) treated with 300 nm SPION-TPP solution, C) treated with 400 nm SPION-TPP solution, and D) treated with 400 nm Rhod-TAT-SPION-TPP solution. After 3 h, the cells were irradiated with light (14 J cm^{-2}), and after 24 h they were stained with the components of the Annexin-V-FLUOS staining kit and analysed by FACS. FL1-H and FL2-H stand for Annexin V FLUOS and propidium iodide (PI) channels, respectively.

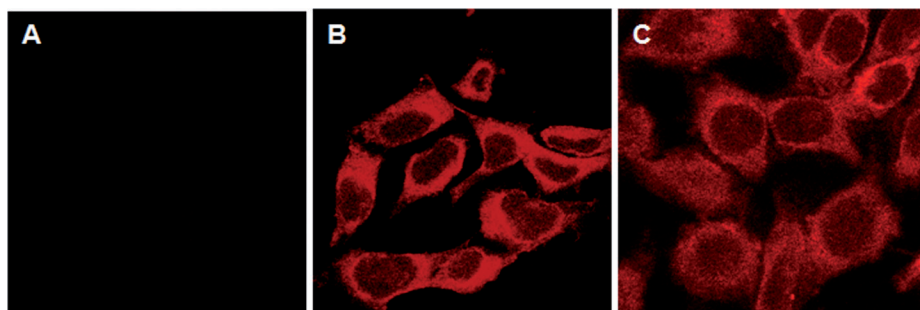


Figure 5. Uptake by confocal laser microscopy. Images of B78-H1 cells untreated (A) and treated with 400 nm Rhod-TAT-SPION-TPP after incubation for 3 h (B) and 24 h (C).

anoma B78-H1 cells, with an IC_{50} value of about 800 nm, whereas they showed no cytotoxicity in the dark.

The bioactivity of SPION-TPP nanoparticles is comparable to that of TPP alone. As anticipated from the singlet-oxygen generation test, the conjugation of TPP to the SPIONs did not alter the $^1\text{O}_2$ production of unbound TPP. Unfortunately, the SPION-TPP nanoconjugate had poor cell penetrability, which affected the linearity of the dose–response effect. Enhanced cell delivery was achieved by conjugating a well-known cell-penetrating peptide (HIV TAT peptide) to the SPION-TPP nanoparticles. The Rhod-TAT-SPION-TPP nanoconjugates showed an improved IC_{50} value of about 500 nm and a linear dose–response effect. Inter-

nalisation of Rhod-TAT-SPION-TPP was confirmed through confocal microscopy by exploiting the rhodamine dye bound to the TAT peptide sequence.

Furthermore, we previously demonstrated through MRI experiments^[23] that TAT-functionalised SPION nanoparticles could lower T2 in labelled HeLa cells, thus functioning as promising contrast agents (see Figure S4 in Supporting Information).

In summary, on the basis of our results, we propose Rhod-TAT-SPION-TPP nanoparticles as promising new theranostic nanoagents: 1) for the treatment of cancer cells by photodynamic therapy (we believe that because of the enhanced permeability and retention effect exhibited by the tumour tissues against high molecular particles, the designed nanoconstructs may show good tumour specificity after blood delivery),^[28] and 2) for the localisation and tracking of therapeutic agents through MRI-based and/or fluorescence-based microscopic techniques.

Experimental Section

Materials and methods: All reagents and solvents were purchased from commercial sources and used as received. Nanomag-D-spio, here referred to as SPION-NH₂ (NH₂ surface, 20 nm; 5 mg mL⁻¹ solid content; 2.4 mg mL⁻¹ iron concentration), was obtained from Micromod Partikeltechnologie GmbH, Germany. 5-(4-Carboxyphenyl)-10,15,20-triphenyl-

21H,23H-porphyrin was purchased from Frontier Scientific Inc., Logan, UT, USA, and the *N*-hydroxysuccinimidyl ester (NHS ester) of 12-azido-4,7,10-trioxadodecanoic acid was obtained from Cyanagen. All other chemicals were obtained from Sigma–Aldrich and were of the highest purity commercially available. TLC analysis was conducted on TLC plastic sheets 60 F254 (Fluka) with detection by UV absorption where applicable and/or by staining with a solution of ammonium molybdate and/or a solution of ninhydrin, followed by charring at approximately 150 °C. Column chromatography was performed using silica gel (0.063–0.200 mm particle size, 70–230 mesh) purchased from Merck. Mass spectra were recorded on an Applied Biosystems/MSD SCIEX QSTAR Hybrid Q-TOF mass spectrometer. ¹H NMR spectra were acquired with a Bruker 200 NMR

spectrometer (200 MHz). Chemical shifts are reported in ppm with tetramethylsilane (TMS) as an internal reference. The abbreviations used are: s=singlet, d=doublet, dd=doublet of doublets, m= multiplet, and br=broad. ¹H-HRMAS-NMR experiments were performed on a Bruker DMX 500 (11.7 T) equipped with an HRMAS ¹H-¹³C indirect detection probe with gradients on the magic angle. MAS experiments were performed at spinning rates up to 8 kHz (15 kHz maximum MAS rotation available) using a 50 μL zirconia rotor. In general, lyophilised nanoconjugate powder (1–2 mg) was dispersed in deuterated DMSO (60 μL). Proton spectra were obtained by using 1024 scans for each experiment. The sample temperature was kept constant at RT.

Synthesis of compound 2: 2-[2-(Boc-amino)ethoxy]ethoxyacetic acid (dicyclohexylammonium salt) **1** (100 mg; 225 μmol) was placed in a round-bottomed flask, and dry DCM (40 mL) was added. EDC (1.2 equiv.; 270 μmol; 52 mg), HOBT-H₂O (1.2 equiv.; 270 μmol; 41 mg), and TEA (2 equiv.; 450 μmol; 63 μL) were added to the solution, which was stirred for 2–3 min. Propargyl amine (1.2 equiv.; 270 μmol; 17 μL) was then added to the mixture, which was stirred overnight. The reaction was monitored by TLC (5% MeOH in DCM). After completion of the reaction, the mixture was evaporated to remove the solvent. The evaporated contents were purified directly by column chromatography (3% MeOH in DCM) without any prior separation. The pure product (57 mg) was obtained as a colourless, viscous liquid in 89.23% yield. ¹H NMR (200 MHz, CDCl₃, 20 °C): δ = 1.36 (s, 9H), 2.21 (t, 2H), 3.28 (dd, 2H), 3.47–3.62 (m, 7H), 3.94 (s, 2H), 4.04–4.00 (dd, 2H), 4.99 (br s, 1H), 7.17 ppm (br s, 1H).

Synthesis of compound 3: Compound **2** (9 mg) was placed in a round-bottomed flask. A 1:1 solution (v/v) of TFA in DCM (10 mL) was added, and the reaction mixture was allowed to stand for 2 h. The solution was evaporated, and this was followed by co-evaporation with toluene (three times) and co-evaporation with TEA (three times). The contents were dissolved in DCM, evaporated, and dried to ensure the removal of volatile components. The product was obtained quantitatively as observed by TLC (5% MeOH in DCM) and used directly for the next step.

Synthesis of compound 4: 5-(4-Carboxyphenyl)-10,15,20-triphenyl-21H,23H-porphyrin (10 mg; 15 μmol), EDC (1.5 equiv.; 23 μmol; 4.4 mg), and HOBT-H₂O (1.5 equiv.; 23 μmol; 3.5 mg) were dissolved in dry DCM. TEA (2.0 equiv.; 30 μmol; 4.2 μL) was added to this solution, which was left to stand for a few minutes. A solution of **3** (1.5 equiv.; 23 μmol; 4.5 mg) dissolved in dry DCM was added, and the reaction mixture was stirred overnight at room temperature. The resulting product was evaporated and purified using column chromatography (4% MeOH in DCM) to obtain 12 mg of pure product. Yield: 94%; ¹H NMR (200 MHz, CDCl₃, 20 °C): δ = -2.79 (s, 2H), 2.26 (t, 1H), 3.60 (dd, 2H), 3.7–3.67 (m, 6H), 4.10 (s, 2H), 4.16–4.12 (dd, 2H), 7.00 (br s, 2H), 7.77 (m, 10H), 8.15–8.36 (overlapping signals, 10H) 8.90–8.77 ppm (overlapping signals, 7H); molecular weight of **4**: 840.34, *m/z* = 841.64 [M + 1]⁺, *m/z* = 686.53 [M-2 phenyl + 1]⁺, *m/z* = 421.82 [(M + 2)]²⁺, *m/z* = 342.76 [M-2 phenyl + 2]²⁺.

Synthesis of SPION-N₃ nanoparticles: The NHS ester of 12-azido-4,7,10-trioxadodecanoic acid (5 mg, 15 μmol) and DIPEA (10 μL) were added to a solution of SPION-NH₂ nanoparticles (Nanomag[®]-D-spio NH₂ surface; 2 mL) in 2 mL of 0.1 M citrate buffer (pH 7.4). The mixture was rotated overnight and then dialysed (SpectraPor regenerated cellulose, 3.5 kDa molecular weight cut-off) against pure water for three to five days to provide SPION-N₃ nanoparticles. The dialysed contents were diluted with deionised water to

a final volume of 10 mL, and this was used as the stock solution of SPION-N₃ for further reactions.

General protocol for copper(I)-mediated “click” chemistry: Compound **4** (2 mg; 2.4 μmol) was dissolved in 10 mM phosphate buffer (500 μL; pH 7.5) (applying first 2 μL of DMSO). Sodium ascorbate (2 equiv.; 4.8 μmol; 0.9 mg) and CuSO₄·5H₂O (0.5 equiv.; 0.3 mg; 1.2 μmol) were added to this solution. Finally, a solution of SPION-N₃ nanoparticles (500 μL) was also added and the reaction mixture was rotated overnight. The resulting solution was dialysed (SpectraPor regenerated cellulose, 3.5 kDa molecular weight cut-off) against 10 mM ethylenediamine tetraacetic acid (EDTA) three times over 12 h, against Milli-Q water for three days, and finally against PBS three times over 12 h as the last step of the process.

Synthesis of Rhod-TAT: The detailed synthetic protocol is described in the Supporting Information, and involves a slight variation of a synthesis published previously by our group.^[23]

ε Measurement by UV spectroscopy: A standard solution of 2 mM TPP in DMSO was prepared. This solution (50 μL) was diluted in 0.5, 1, 1.5, and 2 mL of PBS and the UV absorbance was measured. The experimental value of ε at 422 nm for TPP was obtained by using the Beer–Lambert law, and was calculated to be 1.43 × 10⁵ cm⁻¹ M⁻¹ (SD = 0.45 × 10⁵) as an average of several measurements.

UV/Vis measurements: UV/Vis spectra were measured on a Varian Cary 50 spectrophotometer. Spectra were measured from 200 to 1000 nm, and PBS was used as the baseline (see Figure S1 in Supporting Information). The TPP conjugation on SPIONs was checked through UV/Vis spectroscopy. The Q-band changes were the most significant. Two methods were used to estimate the concentration of TPP loaded on the nanoparticles. One method was based on the correction of the TPP-SPION absorbance (*A*_{TPP-SPION}) by the SPION absorbance (*A*_{SPION}). In this approach, the Beer–Lambert law was applied to Δ*A* = *A*_{TPP-SPION} - *A*_{SPION} at λ_{max} 422 nm (ε = 1.43 × 10⁵ M⁻¹ cm⁻¹, see Figure S1D in the Supporting Information). The second method was based on a designed^[29] deconvolution spreadsheet. This procedure allows the complex absorbance spectrum of TPP-SPIONs to be resolved into individual absorption bands. The peak ascribable to the TPP loaded on SPIONs was calculated directly, and its absorbance value was used to calculate the concentration (see Figure S1A, B, and C in Supporting Information; details of the procedure are also reported there). The concentration values obtained with the two approaches were in good agreement.

Generation of singlet oxygen: ¹O₂ production was evaluated by measuring the time-dependent decay absorbance of the ADPA maximum at 400 nm. A solution of 5-(4-carboxyphenyl)-10,15,20-triphenyl-21H,23H-porphyrin (0.5 μM) containing ADPA (73 μM; total volume 1.2 mL), and a solution of SPION-TPP (0.5 μM) also containing ADPA (73 μM; total volume 1.2 mL) were prepared. A solution of ADPA (73 μM) in PBS (total volume 1.2 mL) was also prepared as a control. All solutions were placed in 24-well plates and irradiated with a Philips halogen bulb (50 W, 12 V).

General preparation for the biological experiments: B78-H1 amelanotic murine melanoma cells were cultured in DMEM (low glucose), which contained 10% fetal calf serum and antibiotics (Penicillin 100 U mL⁻¹, Streptomycin 100 μg mL⁻¹, and Glutamine 2 mM, purchased from CELBIO, Milan, Italy). 5-(4-Carboxyphenyl)-10,15,20-triphenyl-21H,23H-porphyrin, as a positive control, was dissolved in DMSO and conserved in aliquots of 0.5 mM at -20 °C. SPION-TPP and Rhod-TAT-SPION-TPP solutions obtained from dialysis were used as such and diluted in culture medium to the desired concen-

trations. Commercially available SPION-NH₂ nanoparticles were used as negative controls and diluted to a final concentration of Fe comparable to those in the SPION-TPP and Rhod-TAT-SPION-TPP samples.

Cell metabolism assay: B78-H1 cells were seeded in a 96-well plate at a density of 5×10^3 cells/well in 100 μL of culture medium. The following day, the SPION-TPP or Rhod-TAT-SPION-TPP nanoparticles were added at different concentrations, and the cells were incubated in the dark for 3 h at 37 °C and 5% CO₂. This was followed by irradiation with a white halogen lamp (400 WÅm⁻², XEF-152S; San-Ei Electric Co., Ltd) for 30 min (14 Jcm⁻²). A corresponding experiment was performed with treated cells and without light activation. After incubation for 24 h, the cell metabolic activity was evaluated through the resazurin assay, following the manufacturer's instructions (Sigma-Aldrich, Milan, Italy). Data were obtained with a spectrofluorometer Spectra Max Gemini XS (Molecular Devices, Sunnyvale, CA 94089).

FACS analysis: Apoptosis was assessed by using annexin V, a protein that binds to phosphatidylserine (PS) residues, which are exposed on the cell surfaces of apoptotic cells. B78-H1 cells were seeded in a 6-well plate at density of 5×10^5 cells/well. One day later, the cells were treated with SPION-TPP (300 and 400 nm) and Rhod-SPION-TPP (400 nm) nanoparticles for 3 h and illuminated for 30 min (14 Jcm⁻²). After light activation, the cells were washed with PBS, trypsinised, and pelleted. The pellets were suspended in Hepes buffer (100 μL) with annexin V (2 μL) and propidium iodide, PI (2 μL) (annexin-V FLUOS Staining kit, Roche, Penzberg, Germany) and incubated for 10 min at 25 °C in the dark. The cells were analysed immediately through FACS (Becton-Dickinson, San Jose, United States). A minimum of 10,000 cells per sample were acquired in list mode and analysed by using Cell Quest software. The cell population was analysed with FSC light and SSC light. The signal was detected by FL1-H (annexin-V-FLUOS) and FL-2-H (PI). The dual-parameter dot plots combining annexin V-FITC and PI fluorescence show the vial cell population in the lower left quadrant (annexinV-PI), the early apoptotic cells in the lower right quadrant (annexin V-PI), and the late apoptotic or necrotic cells in the upper right quadrant (annexinV-PI).

Confocal microscopy: For investigation of the cellular uptake of the nanoconjugates, 1×10^5 B78-H1 cells were plated on coverslips (diameter 24 mm), and after 24 h, were treated with Rhod-TAT-SPION-TPP (400 nm). Subsequently, after 3 and 24 h, samples were prepared as follows: the cells were washed twice with PBS and fixed with 3% paraformaldehyde (PFA) in PBS for 20 min. After washing with 0.1 M glycine containing 0.02% sodium azide in PBS to remove PFA and Triton X-100 (0.1% in PBS), the cells were incubated with Hoechst to stain the nuclei. Finally, the cells were analysed with a Leica TCS SP1 confocal imaging system (Leica Microsystems, Heidelberg, Germany). Red fluorescence was excited with a 543 nm He-Ne laser and detected with emission bandpass filters of 585/630.

Acknowledgements

We thank Maria Antònia Molins (Institute for Research in Biomedicine, IRB Barcelona, Spain) for her support in recording ¹H HRMAS-NMR data. Emilia Della Pietra and Francesca Simonella are acknowledged for their help during the biological experiments, and Dr. Maurizio Ballico for the ESI-MS measurements. We thank Dr. Milena Acosta, Dr. Silvia Lope-Piedrafita, Dr. Ana Paula

Candiota, and Prof. Dr. Carles Arús (Universitat Autònoma de Barcelona (UAB), Cerdanyola del Vallès, Spain) for their assistance with MRI measurements. Dr. Valentina Mollo and Prof. Dr. Paolo Netti (Italian Institute of Technology@CRIB, Center for Advanced Biomaterials for Health Care, Naples, Italy) are acknowledged for the help with the TEM experiments. This work was supported by "TALENTS for an International House" (co-funded Marie Curie action of AREA Science Park, Trieste, Italy) granted to S.C.; the work done in Barcelona was funded by CICYT (CTQ2012-30930).

Keywords: click chemistry · magnetic properties · photodynamic therapy · porphyrin · superparamagnetic iron oxide nanoparticles

- [1] R. K. Jain, T. Stylianopoulos, *Nat. Rev. Clin. Oncol.* **2010**, *7*, 653–664.
- [2] a) R. Banerjee, Y. Katsenovich, L. Lagos, M. McIntosh, X. Zhang, C.-Z. Li, *Curr. Med. Chem.* **2010**, *17*, 3120–3141; b) C. Corot, P. Robert, J.-M. Idée, M. Port, *Adv. Drug Delivery Rev.* **2006**, *58*, 1471–1504.
- [3] a) J. R. McCarthy, E. Korngold, R. Weissleder, F. A. Jaffer, *Small* **2010**, *6*, 2041–2049; b) J. R. McCarthy, *Nanomedicine* **2009**, *4*, 693–695; c) V. I. Shubayev, T. R. Pisanic, S. Jin, *Adv. Drug Delivery Rev.* **2009**, *61*, 467–477; d) M. Arruebo, R. Fernandez-Pacheco, M. R. Ibarra, J. Santamaría, *Nano Today* **2007**, *2*, 22–32.
- [4] L. LaConte, N. Nitin, G. Bao, *Mater. Today* **2005**, *8*, 32–38.
- [5] M. J. Kogan, I. Olmedo, L. Hosta, A. R. Guerrero, L. J. Cruz, F. Albericio, *Nanomedicine* **2007**, *2*, 287–306.
- [6] a) D. E. Dolmans, D. Fukumura, R. K. Jain, *Nat. Rev. Cancer* **2003**, *3*, 380–387; b) C. H. Sibata, V. C. Colussi, N. L. Oleinick, T. J. Kinsella, *Expert Opin. Pharmacother.* **2001**, *2*, 917–927; c) T. J. Dougherty, *J. Clin. Laser Med. Surg.* **2002**, *20*, 3–7.
- [7] a) T. J. Dougherty, C. J. Gomer, B. W. Henderson, G. Jori, D. Kessel, M. Korbelik, J. Moan, Q. Peng, *J. Natl. Cancer Inst.* **1998**, *90*, 889–905; b) J. B. Miller, *J. Chem. Educ.* **1999**, *76*, 592–594; c) S. Pervaiz, *FASEB J.* **2001**, *15*, 612–617.
- [8] a) V. Vaz Serra, A. Zamarrón, M. A. F. Faustino, M. C. Cruz, A. Blázquez, J. M. Rodrigues, M. G. Neves, J. A. Cavaleiro, A. Juarranz, F. Sanz-Rodríguez, *Bioorg. Med. Chem.* **2010**, *18*, 6170–6178; b) M. C. DeRosa, R. J. Crutchley, *Coord. Chem. Rev.* **2002**, *233*, 351–357.
- [9] a) T. J. Dougherty, *J. Clin. Laser Med. Surg.* **1996**, *14*, 219–221; b) E. D. Sternberg, D. Dolphin, C. Brückner, *Tetrahedron* **1998**, *54*, 4151–4202; c) D. Dolphin, *Can. J. Chem.* **1994**, *72*, 1005–1013.
- [10] a) C. Comuzzi, S. Cogoi, M. Overhand, G. A. Van der Marel, H. S. Overkleef, L. E. Xodo, *J. Med. Chem.* **2006**, *49*, 196–204; b) R. R. Allison, G. H. Downie, R. Cuenca, X.-H. Hu, C. J. H. Childs, C. H. Sibata, *Photodiagn. Photodyn. Ther.* **2004**, *1*, 27–42; c) R. Bonnett, M. C. Barenbaum, *Adv. Exp. Med. Biol.* **1983**, *160*, 241–250.
- [11] a) T. Das, S. Chakraborty, H. D. Sarma, S. Banerjee, M. Venkatesh, *Nucl. Med. Biol.* **2010**, *37*, 655–663; b) E. Zenkevich, E. Sagun, V. Knyukshko, A. Shulga, A. Mironov, O. Efremova, R. Bonnett, S. P. Songca, M. Kassem, *J. Photochem. Photobiol. B* **1996**, *33*, 171–180; c) M. Ballico, V. Rapozzi, L. E. Xodo, C. Comuzzi, *Eur. J. Med. Chem.* **2011**, *46*, 712–720.
- [12] a) S. K. Bisland, D. Singh, J. Garipey, *Bioconjugate Chem.* **1999**, *10*, 982–992; b) L. Chaloin, P. Bigey, C. Loup, M. Marin, N. Galeotti, M. Piechaczyk, F. Heitz, B. Meunier, *Bioconjugate Chem.* **2001**, *12*, 691–700; c) M. Del Governatore, M. R. Hamblin, C. R. Shea, I. Rizvi, K. G. Molpus, K. K. Tanabe, T. Hasan, *Cancer Res.* **2000**, *60*, 4200–4205; d) R. Hudson, R. W. Boyle, *J. Porphyrins Phthalocyanines* **2004**, *8*, 954–975; e) W. M. Sharman, J. E. van Lier, C. M. Allen, *Adv. Drug Delivery Rev.* **2004**, *56*, 53–76; f) G. A. M. S. van Dongen, G. W. M. Visser, M. B. Vrouenraets, *Adv. Drug Delivery Rev.* **2004**, *56*, 31–52.
- [13] a) Y. N. Konan, M. Berton, R. Gurny, E. Allémann, *Eur. J. Pharm. Sci.* **2003**, *18*, 241–249; b) Y. N. Konan, R. Cerny, J. Favet, M. Berton, R. Gurny, E. Allémann, *Eur. J. Pharm. Biopharm.* **2003**, *55*, 115–124; c) J. R. McCarthy, J. M. Perez, C. Brückner, R. Weissleder, *Nano Lett.* **2005**, *5*, 2552–2556; d) I. Roy, T. Y. Ohulchanskyy, H. E. Pudavar, E. J. Bergey, A. R. Oseroff, J. Morgan, T. J. Dougherty, P. N. Prasad, *J. Am. Chem. Soc.* **2003**, *125*,

- 7860–7865; e) F. Yan, R. Kopelman, *Photochem. Photobiol.* **2003**, *78*, 587–591.
- [14] a) M. E. Wieder, D. C. Hone, M. J. Cook, M. M. Handsley, J. Gavrilovic, D. A. Russell, *Photochem. Photobiol. Sci.* **2006**, *5*, 727–734; b) J. R. McCarthy, F. A. Jaffer, R. Weissleder, *Small* **2006**, *2*, 983–987.
- [15] a) M. E. Bakleh, V. Sol, K. Estieu-Gionnet, R. Granet, G. Deleris, P. Krausz, *Tetrahedron* **2009**, *65*, 7385–7392; b) H. Gu, K. Xu, Z. Yang, C. K. Chang, B. Xu, *Chem. Commun.* **2005**, 4270–4272.
- [16] a) R. Huisgen, *1,3-Dipolar Cycloaddition Chemistry, Vol. 1*, Wiley, New York, **1984**; b) R. Huisgen, *Pure Appl. Chem.* **1989**, *61*, 613–628; c) N. J. Agard, J. A. Prescher, C. R. Bertozzi, *J. Am. Chem. Soc.* **2004**, *126*, 15046–15047; d) V. V. Rostovtsev, L. G. Green, V. V. Fokin, K. B. Sharpless, *Angew. Chem.* **2002**, *114*, 2708–2711; *Angew. Chem. Int. Ed.* **2002**, *41*, 2596–2599; e) C. W. Tornøe, C. Christensen, M. Mendal, *J. Org. Chem.* **2002**, *67*, 3057–3064; f) W. G. Lewis, L. G. Green, F. Grynszpan, Z. Radić, P. R. Carlier, P. Taylor, M. G. Finn, K. B. Sharpless, *Angew. Chem.* **2002**, *114*, 1095–1099; *Angew. Chem. Int. Ed.* **2002**, *41*, 1053–1057.
- [17] a) S. N. Goonewardena, H. Zong, P. R. Leroueil, J. R. Baker, *ChemPlusChem* **2013**, *78*, 430–437; b) E. Lallana, A. Sousa-Herves, F. Fernandez-Trillo, R. Riguera, E. Fernandez-Megia, *Pharm. Res.* **2012**, *29*, 1–34.
- [18] J. A. Opsteen, L. Ayres, J. C. M. van Hest, *Material Matters* **2008**, *3*, 62–65.
- [19] C. Wängler, R. Schirmacher, P. Bartenstein, B. Wängler, *Curr. Med. Chem.* **2010**, *17*, 1092–1116.
- [20] a) F. Dumoulin, V. Ahsen, *J. Porphyrins Phthalocyanines* **2011**, *15*, 481–504; b) E. Feese, H. Sadeghifar, H. S. Gracz, D. S. Argyropoulos, R. A. Ghiladi, *Biomacromolecules* **2011**, *12*, 3528–3539; c) M. M. Unterlass, E. Espinosa, F. Boisson, F. D'Agosto, C. Boisson, K. Ariga, I. Khalakhan, R. Charvet, J. P. Hill, *Chem. Commun.* **2011**, *47*, 7057–7059; d) H. Chen, J. Zeng, F. Deng, X. Luo, Z. Lei, H. Li, *J. Polym. Res.* **2012**, *19*, 9880–9889; e) C. Ringot, V. Sol, R. Granet, P. Krausz, *Mater. Lett.* **2009**, *63*, 1889–1891; f) P. K. B. Palomaki, P. H. Dinolfo, *ACS Appl. Mater. Interfaces* **2011**, *3*, 4703–4713; g) S. L. Elmer, S. Man, S. C. Zimmerman, *Eur. J. Org. Chem.* **2008**, 3845–3851.
- [21] a) G. Rousseau, H. Fensterbank, K. Baczko, M. Cano, I. Stenger, C. Larpent, E. Allard, *ChemPlusChem* **2013**, *78*, 352–363; b) G. von Maltzahn, Y. Ren, J.-H. Park, D.-H. Min, V. R. Kotamraju, J. Jayakumar, V. Fogal, M. J. Sailor, E. Ruoslahti, S. N. Bhatia, *Bioconjugate Chem.* **2008**, *19*, 1570–1578; c) A. L. Martin, L. M. Bernas, B. K. Rutt, P. J. Foster, E. R. Gillies, *Bioconjugate Chem.* **2008**, *19*, 2375–2384.
- [22] a) M. J. Pittet, F. K. Swirski, F. Reynolds, L. Josephson, R. Weissleder, *Nat. Protoc.* **2006**, *1*, 73–79; b) M. Lewin, N. Carlesso, C.-H. Tung, X.-W. Tang, D. Cory, D. T. Scadden, R. Weissleder, *Nat. Biotechnol.* **2000**, *18*, 410–414.
- [23] S. Cavalli, D. Carbajo, M. Acosta, S. Lope-Piedrafita, A. P. Candiota, C. Arús, M. Royo, F. Albericio, *Chem. Commun.* **2012**, *48*, 5322–5324.
- [24] L. Polito, M. Colombo, D. Monti, S. Melato, E. Caneva, D. Prosperi, *J. Am. Chem. Soc.* **2008**, *130*, 12712–12724.
- [25] E. Gross, B. Ehrenberg, F. M. Johnson, *Photochem. Photobiol.* **1993**, *57*, 808–813.
- [26] a) C. C. Berry, *Nanomedicine* **2008**, *3*, 357–365; b) H. Brooks, B. Lebleu, E. Vivès, *Adv. Drug Delivery Rev.* **2005**, *57*, 559–577.
- [27] G. Koopman, C. P. M. Reutelingsperger, G. A. M. Kuijten, R. M. J. Keehnen, S. T. Pals, M. H. J. van Oers, *Blood* **1994**, *84*, 1415–1420.
- [28] H. Maeda, *J. Controlled Release* **2012**, *164*, 138–144.
- [29] E. J. Billo, *Excel for Chemists: A Comprehensive Guide*, Wiley, New York, **1997**.

Received: July 29, 2013

Published online on October 23, 2013